

Article

Study on Anti-Weathering Protection of Excavated Ancient Stone Arch Bridge with Nano-Composites

Jian Zhang , Qingwen Ma ^{*}, Xiaowen Zheng, Kaidi Cheng and Ruizhe Lang

School of Water Conservancy and Transportation, Zhengzhou University, Zhengzhou 450001, China; zhangjianzj33@163.com (J.Z.); zwx1875@163.com (X.Z.); zzuckd@163.com (K.C.); 118342940065@126.com (R.L.)
^{*} Correspondence: mqw2008@zzu.edu.cn

Abstract: After archaeological excavation, the underground ancient bridge has changed from a relatively stable underground environment to a modern environment with a large temperature difference between day and night, long sunshine, changeable climate, rain erosion and serious air pollution. In addition to the need to control the external environment, it is necessary to actively carry out research on anti-weathering materials for stone cultural relics. In this study, five common weathering materials were selected, and three of them were hybridized with nano-silica to obtain nano-composites. Through a series of property tests and anti-weathering ability tests, the comprehensive anti-weathering effect of brick samples coated with anti-weathering protective materials was evaluated. The results showed that the composite of nano-silica-methyltrimethoxysilane hydrolysate showed the best comprehensive anti-weathering ability, which provides a certain reference value for the protection of similar masonry cultural relics.

Keywords: masonry cultural relics; anti-weathering materials; nano-silica; methyl trimethoxysilane hydrolysate; microscopic test



Citation: Zhang, J.; Ma, Q.; Zheng, X.; Cheng, K.; Lang, R. Study on Anti-Weathering Protection of Excavated Ancient Stone Arch Bridge with Nano-Composites. *Coatings* **2023**, *13*, 1898. <https://doi.org/10.3390/coatings13111898>

Academic Editor: Enrico Quagliarini

Received: 28 August 2023

Revised: 31 October 2023

Accepted: 3 November 2023

Published: 6 November 2023



Copyright: © 2023 by the authors. Licensee MDPI, Basel, Switzerland. This article is an open access article distributed under the terms and conditions of the Creative Commons Attribution (CC BY) license (<https://creativecommons.org/licenses/by/4.0/>).

1. Introduction

As one of the most common places of interest, ancient bridges witness the rise and fall of history and the development of civilization [1]. Zhouqiao has been deeply buried in the ground because of the flooding of the Yellow River many times in history. The relevant personnel officially started the archaeological excavation of the site of Zhouqiao in 2018. In view of the excavated ancient stone arch bridges similar to Zhouqiao, the sudden change in the occurrence environment is a problem that cannot be ignored. It mainly includes changes in temperature, humidity, light and other conditions, which are also several important factors affecting the weathering speed of the surface of masonry cultural relics [2,3].

At present, studies on bridge protection primarily focus on the load-bearing capacity. Generally, the structural response of the bridge is predicted and analyzed by means of numerical simulation and deformation monitoring, so as to guide the reinforcement and protection of the bridge. As an excavated ancient bridge, Zhouqiao no longer serves as a transportation route. However, as a valuable cultural relic, the information preserved on its surface is of great significance. Therefore, conducting research on anti-weathering protection is particularly important.

The traditional anti-weathering reagents are mainly inorganic materials, and the reinforcement mechanism is that some substances in the materials react or hydrate with CO₂; the products fill the pores [4], but the connection between the products and minerals is weak. In addition, inorganic materials make it easy to form incompatible hard shells on the surface and break into small pieces. At the same time, there are some problems such as irreversibility and panalkali [5–7], which are not suitable for cultural relic protection. There are many kinds of organic anti-weathering materials commonly used in modern times, mainly including natural and synthetic polymers. Each kind of material has its own unique

advantages. Acrylic resin has the characteristics of stability, colorless transparency and good flexibility [8], but it also has some problems, such as becoming soft and sticky in summer and hard and brittle in winter. At present, scholars mostly make up for the deficiency of the material itself by modifying it [9,10]. Silicone materials have many advantages, such as water resistance, air permeability, ultraviolet aging resistance, good permeability and environmental protection, etc. The hydroxyl group in siloxane structure makes it have great research potential in the field of preparing new composite materials [11–13]. Generally speaking, a single organic and inorganic material has some shortcomings in the field of masonry cultural relics protection. The difference of molecular structure leads to the different performance of organic and inorganic materials [14]. Therefore, by combining the advantages of organic and inorganic materials, we can achieve the effect of learning from each other [15,16]. Through the combination of organic and inorganic materials at the nanometer level, the protective performance can be further improved, and the application scenarios can be broadened.

Aslanidou [17] added nano-SiO₂ particles with a particle size of 7 nm to alkoxysilane and sprayed the mixed solution on marble and sandstone samples. The results show that the nanoparticles construct a uniform and rough surface, and the proper concentration of nano-particles can give the composite coating a superhydrophobic performance. Victor Fruth [18] added magnesium oxide and titanium dioxide nanoparticles to sodium polyacrylate (NaPAC), and the obtained coating showed good hydrophobicity, negligible color change and self-cleaning characteristics of degrading dyes under ultraviolet irradiation. Peng [19] modified dodecyl trimethoxysilane (DTMS) with nano-TiO₂ and nano-SiO₂ particles, both of which improved the hydrophobicity, ultraviolet radiation resistance and thermal stability of the basic material. After the DTMS was modified by the two nanoparticles together, the obtained composite material had excellent hydrophobicity, low discoloration and outstanding durability; it also retained the water vapor permeability of stone of about 85%, showing that various nanoparticles were used in stone. Wang [20] modified fumed nano-SiO₂ with isobutyl triethoxysilane with the sol-gel method at room temperature. The composite coating has strong antifouling and self-cleaning effects, excellent thermal stability and artificial aging resistance, and excellent weather resistance. Shu [21] dispersed anatase nano-titanium dioxide particles into titanium dioxide sol to prepare nano-composite sol materials, which showed good air permeability and photocatalytic performance, which could greatly improve the weather resistance of the protected objects and reduced the erosion of soluble salt.

Traditional organic and inorganic protective materials have been verified by long-term practice and can be used in the protection project of masonry architectural heritage in specific scenes. However, the shortcomings of traditional protective materials are also very prominent, and it is difficult to be used in a wider and more complex natural environment. In particular, the erosion of outdoor cultural relics by various urban pollutants has gradually attracted people's attention, highlighting the urgent need for research, development, and application of new protective materials [22]. The strategy of dispersing inorganic nanoparticles in organic materials to prepare composite coatings has the advantages of economy, environmental protection and convenient operation. In addition, different nanoparticles can impart special properties to composite coatings, thereby creating a wide range of research opportunities in functional materials [23–25].

In this paper, the existing masonry at the Zhouqiao site is taken as the research object, and five representative protection materials are selected from the common anti-weathering materials of masonry cultural relics. After gaining a general understanding of the performance characteristics of the representative materials, three of them are selected as the basic materials for the experimental doping of nano-materials. Through a series of tests, the actual protective effects of the five representative materials and nano-composites were comprehensively evaluated; according to the test results, the materials with the best comprehensive protective effects were selected. Through SEM and XRD tests, the changes in micro-morphology and mineral composition of the bricks after coating with weathering

materials are explored from the microscopic point of view. This is performed in order to obtain a new anti-weathering material with better comprehensive ability on the basis of previous studies and provide references for the anti-weathering protection of the Zhouqiao site and similar masonry cultural relics.

2. Materials and Methods

2.1. Materials and Sample Preparation

2.1.1. Present Situation of the Zhouqiao Site

The Zhouqiao site is located in Gulou District, Kaifeng City, Henan Province. It is situated in the middle and lower reaches of the Yellow River and belongs to the alluvial plain of the Yellow River. The soil consists mainly of clay and sand. The average temperature in the hottest month in Kaifeng is 32.1 °C, with an average outdoor relative humidity of 79%. In the coldest month, the average temperature drops to −3.5 °C, with an average outdoor relative humidity of 64%. The stable groundwater level is found at a buried depth of 4.5–7.4 m.

Figure 1a shows the archaeological excavation site. The slightly protruding Zhouqiao in the figure is confirmed to be a bridge that was rebuilt during the Ming Dynasty. It is a single-arch stone bridge paved with bluestone, measuring 25 m in length from north to south and 30 m in width from east to west. The hole is 6.58 m tall and 5.8 m wide. Figure 1b shows a large-scale stone mural on the riverbank, which dates back to the Song Dynasty. The mural covers an area of over 330 square meters, featuring vibrant patterns of seahorses, cranes and auspicious clouds. The carved stone is 3.3 m tall and has a total length of over 30 m. It consists of 16 floors, making it of significant archaeological research value.



(a)



(b)

Figure 1. Photos of the Zhouqiao site: (a) The archaeological excavation site; (b) The riverbank stone carving murals.

At present, there are some major diseases in the ontology of the Zhouqiao site, such as structural instability, partial deformity, surface weathering, biological breeding (Figure 2), etc. The structural problems can be temporarily solved by physical measures, but if the weathering problems are not handled in time, it will seriously affect the preservation of its surface cultural information, which is very fatal to archaeological research. Therefore, it is necessary and urgent to reduce the weathering effect of external environmental conditions such as temperature, humidity, light and biology on the Zhouqiao body.

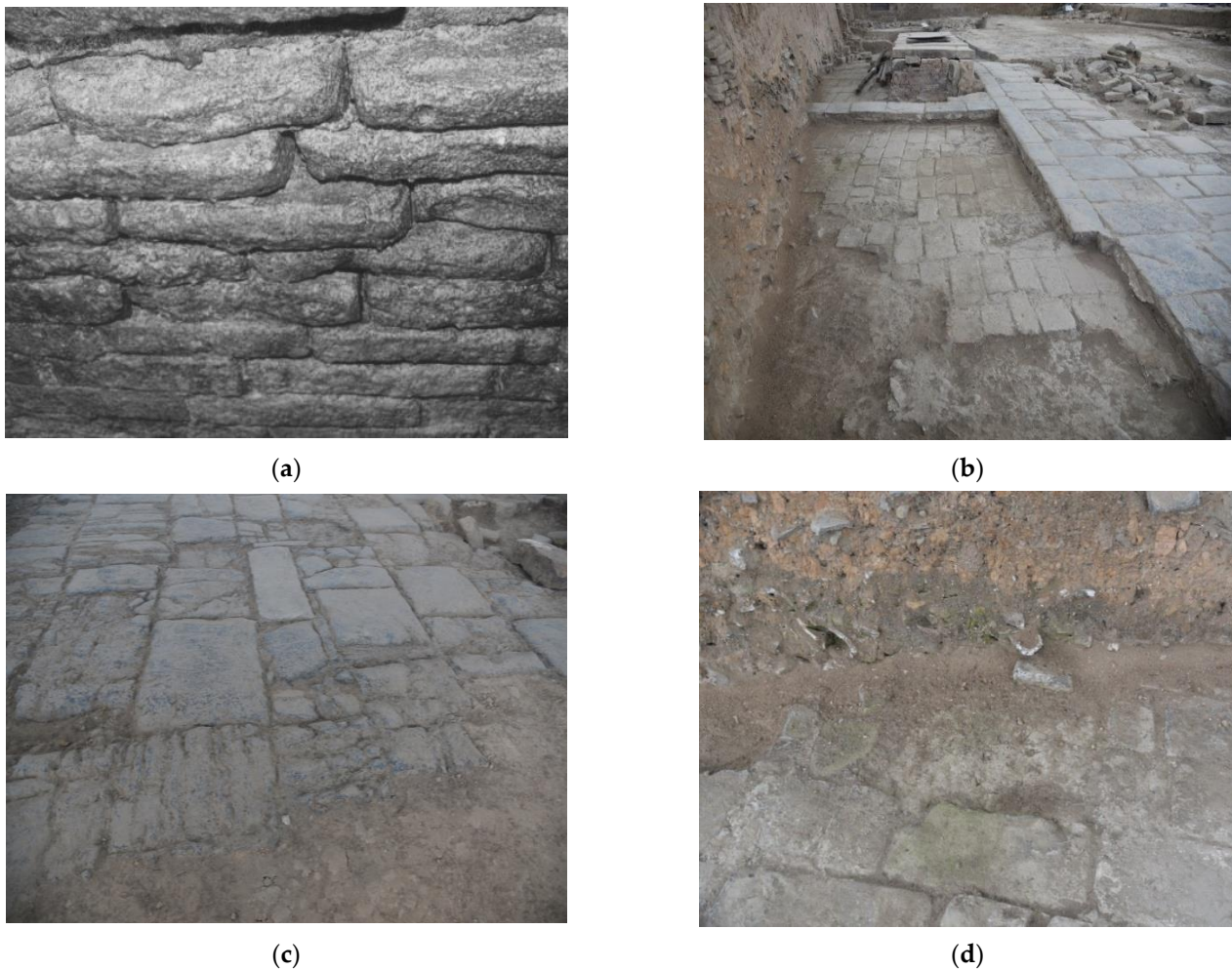


Figure 2. The main diseases existing in Zhouqiao site: (a) Structural instability; (b) Partial deformity; (c) Surface weathering; (d) Biological breeding.

2.1.2. Materials

Small bricks to be coated

In this paper, the damaged bricks at the Zhouqiao site were selected as the experimental protection object. The large bricks were cut into small cubes of 25 mm × 25 mm × 10 mm by a wire cutting machine and polished with 80 mesh sandpaper. Then, the small bricks were washed with distilled water to remove the possible stains during cutting and polishing. Finally, the small bricks were put into a blast drying oven, and the temperature was set to 60 °C; the small bricks were dried for later use. The damaged bricks on the bridge deck and the finished small bricks are shown in Figure 3.

Experimental materials

All the experimental materials needed for this study are listed in Table 1.

In addition, methyl trimethoxysilane, anhydrous ethanol and distilled water were mixed at a volume ratio of 10:10:1, the temperature was controlled below 45 °C, and the mixed solution was allowed to fully hydrolyze for five hours to prepare methyl trimethoxysilane hydrolysate.



Figure 3. (a) Damaged bricks; (b) Small bricks to be coated.

Table 1. Experimental materials.

Material	Manufacturer
Potassium methyl silicate	Shandong Xingchi Chemical Co., Ltd., Jinan, China
Waterborne acrylic emulsion	Shenzhen Jitian Chemical Co., Ltd., Shenzhen, China
Methyl trimethoxysilane	Runyou Chemical Co., Ltd., Shenzhen, China
Nano-silica particles	Hebei Zhongye New Material Co., Ltd., Xingtai, China
Nano-titanium dioxide sol (MTI-2080)	Qianhai Jishengya Technology Co., Ltd., Shenzhen, China
Sodium tripolyphosphate ($\text{Na}_5\text{P}_3\text{O}_{10}$)	Shanghai Xintai Industrial Co., Ltd., Shanghai, China
Anhydrous sodium sulfate	Tianjin Zhiyuan Chemical Reagent Co., Ltd., Tianjin, China
Sodium hydroxide solution	Guangzhou Cishui Technology Co., Ltd., Guangzhou, China
Dilute sulfuric acid solution	Jiangyin Marvel Chemical Co., Ltd., Jiangyin, China

2.1.3. Sample Preparation

The selection of several representative anti-weathering materials from a wide range of materials as the basic materials for this study should be conducted based on the following principles: choosing from the anti-weathering materials of masonry cultural relics that have been previously studied; selecting based on different types and compositions of materials; excluding anti-weathering materials that are not suitable for this study based on known characteristics or conducting basic property tests; and considering the cost-effectiveness of the materials.

In this study, five kinds of anti-weathering organic materials were selected as the basic materials (A–E) based on the aforementioned principles, as shown in Table 2. In addition, based on the preliminary screening test results of these five basic materials, three of them (A, D and E) with better effects were selected for doping with nano-silica, and three kinds of nano-composites (F–H) were obtained, as shown in Table 3. Simultaneously, a control group (I) and a blank group (X) were set up for the tests.

Table 2. Basic materials.

Number	Material	Material Properties
A	Potassium methyl silicate (Alkaline organosilicate)	common waterproofing agent, corrosion resistance [26,27]
B	Waterborne acrylic emulsion (High polymer)	good permeability, film forming [28,29]
C	Methyl trimethoxysilane (Organosilicon)	good air permeability, hydrophobicity, aging resistance, good reinforcement effect [30,31]
D	Methyl trimethoxysilane hydrolysate	same as above
E	Nano-titanium dioxide sol (MTI-2080) (Nano-material)	high transparency, ultraviolet radiation resistance, good photocatalysis, air permeability [21]

Table 3. Nano-composites, control group and blank group.

Type	Number	Material
Nano-composites	F	Potassium methyl silicate + 0.5%Nano-SiO ₂
	G	Methyl trimethoxysilane hydrolysate + 0.5%Nano-SiO ₂
	H	Nano-titanium dioxide sol (MTI-2080) + 0.5%Nano-SiO ₂
control group	I	Distilled water + 0.5%Nano-SiO ₂
blank group	X	Distilled water

Separate brushes were used to coat the above ten groups of materials on the small bricks, each time ensuring that the six sides of the bricks were evenly covered by the materials. After that, the coated samples were placed in a blast drying oven, and the temperature was set at 60 °C and dried for five minutes. After removing from the oven, the materials were coated for the second time; this was repeated three times. Ten groups of samples coated with ten groups of materials were prepared.

Among them, a proper amount of Na₅P₃O₁₀ (dispersant) should be added to the nano-composites, and the nano-composites should be mechanically stirred and dispersed by an electric stirrer for later use.

2.2. Testing Methods

On the basis of previous studies, combined with the occurrence environment of the Zhouqiao site, the following nine groups of experiments or tests have been carried out in this study, which can reflect the anti-weathering ability of materials to some extent.

The instruments used in the experiment are listed in Table 4.

Table 4. Statistical table of test instruments.

Instruments	Manufacturer and Model
Scanning electron microscope (SEM)	FEI, Hillsboro, OR, USA, QUANTA-650
X-ray diffraction analyzer (XRD)	Brooke company, Karlsruhe, Germany, D8 ADVANCE
Electric mixer	Putian Instrument Manufacturing Co., Ltd., Changzhou, China, JJ-1
Ultraviolet high-pressure pump lamp	Changya Lighting Electric Co., Ltd., Wuxi, China, GGY250W
Electric heating air-blast drying oven	Sunne, Shanghai, China, 101-00A
Spectrophotometer	Taisite, Tianjin, China, V721
Colorimeter	Linshang Technology Co., Ltd., Shenzhen, China, LS170

2.2.1. Material pH Test

The pH of anti-weathering materials was determined using pH test paper. Excessive acidity or alkalinity of protective materials can have detrimental effects on cultural relics.

2.2.2. Color Difference Test

The coating of anti-weathering materials cannot cause great changes in the external morphology of masonry cultural relics. One of the important principles is that the color difference (ΔE) between the relics before and after protection cannot be too large [32]. According to the trichromatic principle, the chromaticity of sample's appearance can be determined based on its lightness (L^*), red/green opponent colors (a^*) and yellow/blue opponent colors (b^*). The chromaticity of the sample coated with different anti-weathering materials is measured by the LS170 colorimeter. Five groups of samples were determined for each material, and the average value was calculated from the results. The calculation method of the color difference (ΔE) is shown in the following formula (1) [33]. When $\Delta E \geq 5$, it is considered that the color difference between the sample before and after the coating is too large.

$$\Delta E = \sqrt{(\Delta L^*)^2 + (\Delta a^*)^2 + (\Delta b^*)^2} \quad (1)$$

In the formula, ΔL^* , Δa^* and Δb^* indicate the difference of CIE-L*a*b* coordinates (chromaticity coordinate system) before and after the sample was coated with materials.

2.2.3. Salt Resistance Cycling Test

The ten group samples were dried for 24 h and cooled to room temperature, and the initial mass of the samples was recorded as M_0 . The samples were put evenly in the water tank at intervals, 10% sodium sulfate solution was added into the water tank, the samples were soaked in the solution for 24 h, and then put in a drying oven for 24 h. The surface color change, color, pulverization and cracking were observed, and their mass was measured. The above process was carried out for 14 cycles (28 days), and the mass after the n th cycle was recorded as M_n . Every cycle, calculate the mass change rate (ω_n) of each group of samples. The formula of mass change rate is shown in formula (2) [34].

$$\omega_n = \frac{M_n - M_0}{M_0} \times 100\% \quad (2)$$

2.2.4. Water Absorption and Air Permeability

Water is one of the main factors that affects the weathering of masonry cultural relics, so it is important to control water-related properties of the material. It is an important aspect to test whether the protective material is effective or not to test the waterproof property of the protected sample. According to the experimental conditions and current testing methods, the waterproof effect of the protective material is mainly studied by comparing the water absorption of the coated samples with that of the blank sample. This test process is carried out with reference to the Evaluation Method of Protective Effect of Weathering Materials for Sandstone Cultural Relics [35].

Permeability refers to the ability of water vapor to evaporate through the pores of a rock mass, which reflects the rock's ability to breathe. In the screening of anti-weathering materials, it is required that the materials have adequate air permeability to ensure that the water within the stone can interact with the outside world through steam after the materials are coated. This experiment was carried out according to the method mentioned in the Test Method for Water Vapor Permeability of Building Materials and Their Products [36]. When measuring the air permeability, a proper amount of distilled water was poured into a plastic bottle with a diameter slightly smaller than the width of the sample, and then, the sample was bonded to the plastic bottle with glass glue and fully sealed. The permeability is characterized by the ratio of water reduction to the initial mass.

2.2.5. Ultraviolet Radiation Resistance Test

Anti-weathering materials will be irradiated by light in the process of use, and these materials will induce a photo-oxygen reaction under the irradiation of ultraviolet rays, which will lead to the aging of anti-weathering materials and the degradation of their properties [37]. In this experiment, the ultraviolet radiation resistance of each anti-weathering material is evaluated by the color difference of the sample after accelerated aging by ultraviolet radiation and the ultraviolet absorption and shielding ability of the material itself.

1. Sample Aging Test

The artificial accelerated aging resistance test was carried out according to the GB/T 1865-2009 standard [38]. The sample was placed under the irradiation of a 250 W ultraviolet high-pressure pump lamp, which mainly radiated ultraviolet with the wavelength of 365 nm. The sample was 20 cm away from the lamp, and the temperature was room temperature. After 250 h, the quality, color and surface morphology of the sample were observed.

2. Transmission Ratio Test

A proper amount of materials was added into a 1 cm standard glass cuvette, different wavelengths were selected, the transmittance of the standard black block was adjusted to 0%, and the transmittance of the blank area was adjusted to 100%. The transmittance of

different anti-weathering protection materials was tested at wavelengths of 350–500 nm, and the transmittance was measured with a spectrophotometer.

2.2.6. Microscopic Test

The microstructure characteristics of materials can be clearly observed through SEM images. Small pieces were cut from the whole sample as observation samples, and the conductivity of the observation samples was enhanced by winding conductive adhesive and gold-plated film on the surface. After the gold spraying was completed, the samples were put on the test bench to be scanned and observed for their microscopic characteristics. The blank group sample X, sample D coated with methyl trimethoxysilane hydrolysate, and sample G coated with 0.5% nano-silica-methyl trimethoxysilane hydrolysate hybrid were observed, and the magnifications of the test were 200, 500, 1000, and 2000 times.

The mineral composition of rock mass is one of the main factors affecting the material structure characteristics of rock mass, and it is also an important basis for determining the physical characteristics of rock mass. The main mineral composition of the sample can be determined by the XRD test, which uses primary X-ray photons or other microscopic particles to excite atoms in the substance to be detected to generate fluorescence (secondary X-ray) and obtain diffraction patterns to analyze the substance composition. The blank sample X and the sample G coated with 0.5% nano-silica-methyltrimethoxysilane hydrolysate were tested, and the scanning angle of the instrument was set at 0–80°, which basically reflected all the mineral components contained in the sample.

3. Results and Discussion

3.1. Material pH Test Results and Analysis

The pH test results for all anti-weathering materials are shown in Table 5.

Table 5. pH value of each material.

Number	Material	pH Value
A	Potassium methyl silicate	10
B	Waterborne acrylic emulsion	8
C	Methyl trimethoxysilane	7
D	Methyl trimethoxysilane hydrolysate	7
E	Nano-titanium dioxide sol (MTI-2080)	2
F	Potassium methyl silicate + 0.5%Nano-SiO ₂	10
G	Methyl trimethoxysilane hydrolysate + 0.5%Nano-SiO ₂	7
H	Nano-titanium dioxide sol (MTI-2080) + 0.5%Nano-SiO ₂	2
I	Distilled water + 0.5%Nano-SiO ₂	7
X	Distilled water	7

The test results show that potassium methylsilicate is slightly alkaline, and nano-titanium dioxide sol shows strong acidity. From the point of view of the acidity and basicity of materials, these two materials cannot meet the neutral requirements of anti-weathering protection materials, and the pH values of waterborne acrylic emulsion, methyl trimethoxysilane, and methyl trimethoxysilane hydrolysates are moderate. It will not cause damage to masonry relics because of its strong acidity and alkalinity. At the same time, the addition of nano-materials has no significant effect on the pH of the base materials.

3.2. Color Difference Test Results and Analysis

The results of the color difference measurement of samples before and after coating with ten materials are shown in Table 6.

Table 6. Color difference of samples before and after coating of each material.

Sample Number	ΔL^*	Δa^*	Δb^*	ΔE
A	−10.974	0.314	1.784	11.192
B	−19.764	0.626	2.558	19.924
C	−1.874	0.988	0.480	2.768
D	−3.438	0.134	0.630	3.694
E	−5.310	0.332	0.164	5.426
F	−8.618	−0.166	1.636	8.798
G	−0.414	0.426	−1.612	2.736
H	−3.118	0.278	−1.138	3.644
I	1.424	−0.502	−1.348	2.336
X	−0.194	0.038	−0.092	0.586

Among the five basic materials, the color difference of potassium methylsilicate (effective component 40%) and waterborne acrylic emulsion before and after coating is larger, and the color difference of nano-titanium dioxide sol before and after coating is slightly larger. After coating, the lightness of the sample is greatly reduced. Therefore, dilution or a small amount of additives should be considered when these three materials are used separately as anti-weathering protective materials.

Potassium methylsilicate, methyltrimethoxysilane (hydrolysis), and nanometer titanium dioxide sol can reduce the color difference of the samples before and after coating. It can be considered that for materials with a large decrease in lightness after coating, the addition of an appropriate amount of nano-silica can reduce the color difference. This is because nano-silica has the ability to reflect visible light [39], which results in a shinier appearance of the sample after coating the material.

3.3. Salt Resistance Cycling Test Results and Analysis

The appearance changes of ten groups of samples after the first and fourteenth salt tolerance cycles are shown in Figure 4. The quality changes of ten groups of samples in 14 salt tolerance cycle tests are shown in Figure 5.

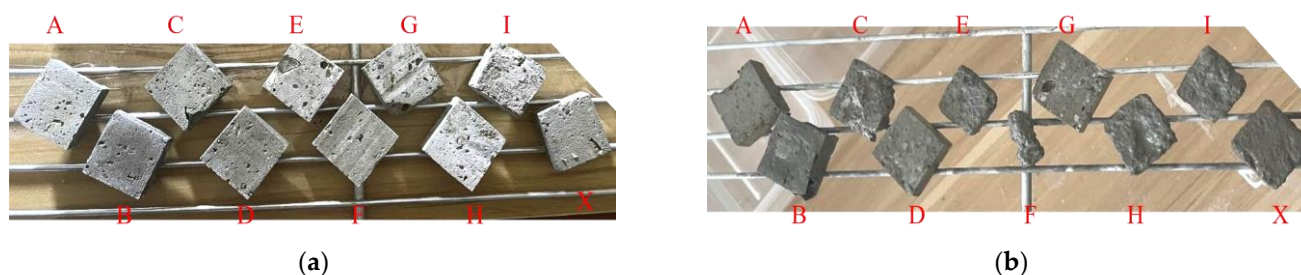


Figure 4. Appearance changes of A–I group and blank group samples in salt resistance cycling test (From left to right is A to I, and the rightmost is X): (a) Samples after the first salt tolerance cycling test; (b) Samples after the fourteenth salt tolerance cycling test.

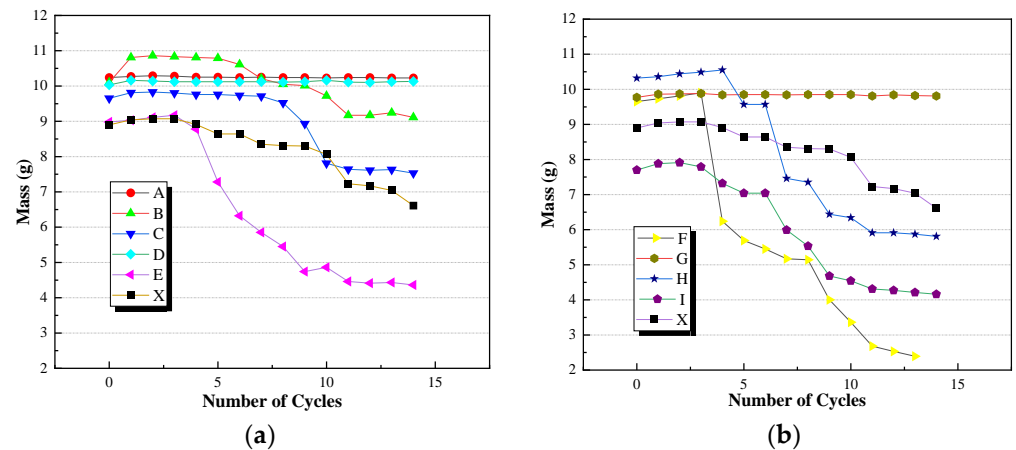


Figure 5. Mass change of samples in salt tolerance cycling test: (a) A–E group samples and blank group sample (X); (b) F–I group samples and blank group sample (X).

As can be seen from Figure 5, during the salt tolerance cycle, the mass of ten groups of samples showed a trend of slightly increasing at first and then decreasing. Among them, the mass change of blank group X shows a uniform decrease. The quality of the sample in group B was relatively stable in the first five cycles, but a small amount of peeling occurred in the sixth cycle. Through observation, the sample formed a hard shell of about 1–2 mm on the outermost layer, and there was almost no caustic soda on its surface, but its interior was gradually eroded, as shown in Figure 6a; The mass changes of the four groups E, F, H, and I are greater than that of the blank group X, among which the three groups F, H, and I are materials doped with nano-silica, and they have obvious cracking and peeling phenomena in the salt-resistant cycle, as shown in Figure 6b. In the salt-resistant cycle test, the possible reasons for the accelerated failure of the sample caused by the above materials are as follows.



(a)



(b)

Figure 6. The material treatment interface: (a) Appearance changes of group B sample; (b) Appearance changes of group F sample.

- The anti-weathering material itself has insufficient permeability.

After brushing, the materials cannot completely penetrate into the sample, and the samples treated with these materials will form a “material treatment interface”, which means that only the outside of these groups of samples is protected by the materials. The hydrophobicity of the infiltrated area of these materials is different from that of the non-

infiltrated area, which leads to the formation of a “dry–wet interface” at the “material treatment interface”. During the test, salt will gather at the “dry–wet interface” inside the sample. With the periodic change of temperature and humidity, mineral particles will expand and contract repeatedly, resulting in a large stress difference at the “dry–wet interface”, which accelerates the destruction of the sample.

- The outer hard shell peeled off in a large area.

Because of the infiltration of materials on the surface, the outer layer of the samples formed a hard shell as a whole. Compared with the blank group, these samples are more likely to peel off the outer hard shell in a large area during the test, while the blank group usually only causes the surface layer to erode little by little, even if there are a few cracks. Therefore, in the mass change curve, the curves of these groups of samples showed a “cliff” decline.

- Reverse migration phenomenon.

Some organic anti-weathering protective materials will exhibit a “reverse migration phenomenon” due to the volatilization of solvents after coating, which affects the penetration depth of the materials.

In this test, three groups of materials with better performance were A, D and G. The mass of group A decreased slightly, while the mass of groups D and G increased slightly. Their mass change rate was less than 1%. Compared with the blank group X, salt tolerance improved significantly. This is basically consistent with the experimental results of Wan [34]. Compared with the results of C, D and G groups, it is found that the salt tolerance of methyltrimethoxysilane can be greatly improved after hydrolysis. This improvement may be due to the condensation reaction between the silyl alcohol formed after hydrolysis and the active hydroxyl group of the sample. This reaction forms -Si–O–Si- bonds, which connect the weathered loose particles for the purpose of reinforcement. And, the addition of nano-silica did not reduce the salt tolerance of methyl trimethoxysilane hydrolysate.

3.4. Water Absorption Test Results and Analysis

According to the water absorption test method, the water absorption of ten groups of samples was measured, and the specific results are shown in Table 7.

Table 7. Water absorption of each group of samples.

Sample Number	Water Absorption (%)	Sample Number	Water Absorption (%)
A	17.83	F	15.98
B	19.44	G	3.48
C	18.48	H	20.28
D	2.90	I	25.11
E	19.87	X	25.03

It can be seen from Table 6 that, except for group I, the water absorption of the other eight groups of samples is lower than that of the blank group, indicating that the weathering protection materials selected in the primary and the materials compounded with nano-silica played a certain waterproof effect. However, the samples in group B (waterborne acrylic emulsion) showed obvious whitening after soaking in the flume for 24 h, which seriously affected the original appearance of the sample; the samples in group E (nano-titanium dioxide sol) showed slight whitening after soaking in the flume for 24 h, and the appearance of the other groups had no obvious change.

The water absorption of group A (potassium methylsilicate), group C (methyl trimethoxysilane), and group D (methyl trimethoxysilane hydrolysate) was significantly lower than that of the blank group. The decrease in water absorption of the samples in groups C and D may be related to the inert hydrophobic group. Alkylsiloxane can be expressed by the general formula of the inert hydrophobic group ($R_nSi(OX)_{4-n}$), in which the inert hydrophobic group (R_n) makes it more difficult for water to permeate into the sample.

The water absorption of the sample slightly increases after the nano-materials are doped. This is because hydrophilic hydroxyl groups attach to the surface of silica nanoparticles, and the presence of these hydroxyl groups enhances the ability of water to enter the pores [40,41].

3.5. Air Permeability Test Results and Analysis

The overall mass of the sample, container, glass glue and distilled water in the bottle changes with time as shown in Figure 7.

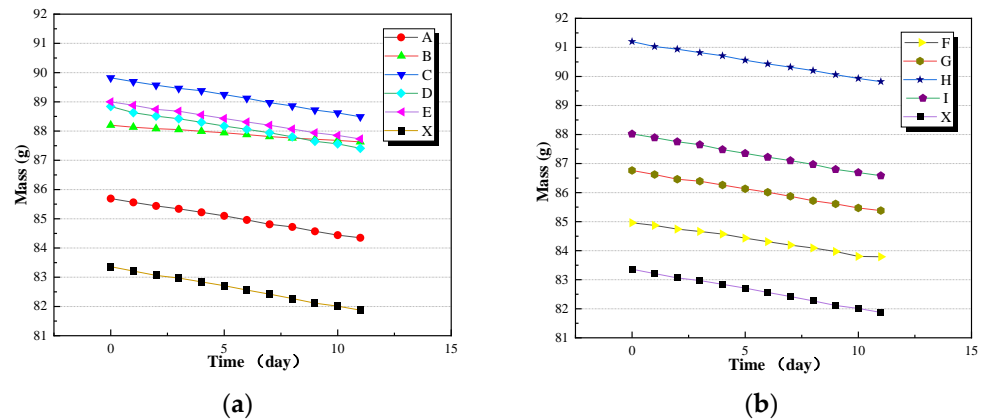


Figure 7. Curve of total mass changing with time in the air permeability test: (a) A–E group samples and blank group sample (X); (b) F–I group samples and blank group sample (X).

Comparing the data of the 11th day with the blank group, the decrease of less than 10% is excellent, 10%–20% is good, 20%–30% is medium, and if the drop value is greater than 30%, it means that the air permeability is extremely bad [42].

The evaluation of the air permeability of each group of samples is shown in Table 8.

Table 8. Evaluation of air permeability of each group of samples.

Sample Number	Initial Mass (M ₀ /g)	11th Day Mass (M ₁ /g)	Poor Mass (g)	Air Permeability (%)	Rate of Decline (%)	Air Permeability Evaluation
A	84.96	83.79	1.17	1.38	22.96	medium
B	88.2	87.63	0.57	0.65	63.84	bad
C	89.82	88.49	1.33	1.48	17.16	good
D	86.76	85.38	1.38	1.59	11.01	good
E	89.00	87.73	1.27	1.43	20.17	medium
F	85.69	84.35	1.34	1.56	12.51	good
G	88.84	87.41	1.43	1.61	9.95	excellent
H	91.20	89.82	1.38	1.51	15.34	good
I	88.02	86.48	1.54	1.75	2.17	excellent
X	83.36	81.87	1.49	1.79	/	/

Compared to the blank group, the air permeability of the samples coated with the anti-weathering protective material is reduced. This is because the coating materials penetrated the samples and filled some of the pores, which worsened their permeability. The air permeability of the sample in group G (nano-silica-methyltrimethoxysilane hydrolysate) is the best, and it only experiences a reduction of less than 10% compared to the blank group. Compared to group C (methyl trimethoxysilane), the air permeability of group D (methyl trimethoxysilane hydrolysate) is somewhat improved. Group B sample (waterborne acrylic emulsion) exhibits the poorest air permeability. This can be attributed to the formation of a dense film on the sample’s surface after the application and drying of the water-borne

acrylic emulsion. This film acts as a barrier, preventing the interaction between the water inside the bricks and the external environment.

The enhancement of air permeability in the samples coated with three groups of composite materials may be attributed to the inclusion of suitable dispersant during the material preparation.

3.6. Ultraviolet Radiation Resistance Test Results and Analysis

1. Sample Aging Test

The mass and color changes of the samples after 250 h of irradiation under the ultraviolet high-pressure pump lamp are shown in Table 9.

Table 9. The mass and color changes of the samples.

Sample Number	Mass Change (g)	ΔL^*	Δa^*	Δb^*	Δ
A	−0.01	1.40	0.22	−0.16	1.43
B	−0.02	0.63	−0.14	−0.47	0.80
C	0.00	0.44	0.17	0.57	0.74
D	0.00	0.59	0.47	−0.16	0.77
E	0.03	−1.71	−0.58	0.60	1.90
F	0.01	1.96	−1.54	0.68	2.58
G	0.00	0.47	−0.17	−0.23	0.55
H	0.04	0.18	−0.90	0.82	1.23
I	−0.02	1.38	−0.11	−0.99	1.70
X	0.01	−0.10	−1.19	−0.19	1.21

After 250 h of ultraviolet irradiation, the mass of the sample has hardly changed, and the color difference is difficult to be detected with the naked eyes. Among them, the three groups of samples with the least influence after ultraviolet irradiation are C (methyl trimethoxysilane), D (methyl trimethoxysilane hydrolysate) and G (nano-silica-methyl trimethoxysilane hydrolysate composite), and the addition of nano-silica particles has no obvious effect on the color difference of samples before and after ultraviolet aging.

2. Transmission Ratio Test

Figure 8 shows the transmission ratio of five groups of materials A, C, D, E, G and X (distilled water) under ultraviolet light (350 nm and 365 nm) and visible light (400 nm, 450 nm, 500 nm and 550 nm).

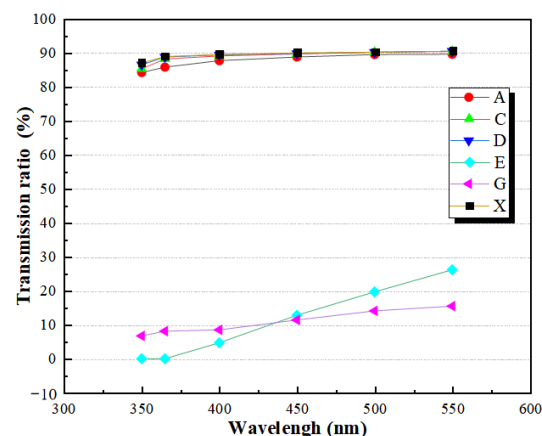


Figure 8. The curve of the transmission ratio with the wavelength of light.

Potassium methylsilicate, methyl trimethoxysilane, and methyl trimethoxysilane hydrolysate have a high transmission ratio, which indicates that these three materials have

good light transmittance. Group E has the lowest transmittance in the ultraviolet wavelength range, and its transmittance is gradually higher than that of group G with the increase of wavelength in the visible wavelength range. Comparing the results of group D and group G, it can be found that after doping with 0.5% nano-silica, the transmittance of the material decreased significantly, and its transmittance decreased by 90.89% under 365 nm ultraviolet light, indicating that the nano-composite showed stronger shielding and absorption performance for ultraviolet light than a single organic anti-weathering material.

The addition of nano-silica enhances the ultraviolet resistance of the composites, which is similar to the result obtained by Li [43].

3.7. Microscopic Test Results and Analysis

1. Scanning Electron Microscope Test

In Figure 9a–c are the micro-morphology diagrams of the blank group sample, the sample coated with methyl trimethoxysilane hydrolysate and the sample coated with nano-silica-methyltrimethoxysilane hydrolysate composite under 500 times magnification with the scanning electron microscope; Figure 9d–f shows the micro-morphology diagrams of the three groups of samples under 2000 times magnification with the scanning electron microscope.

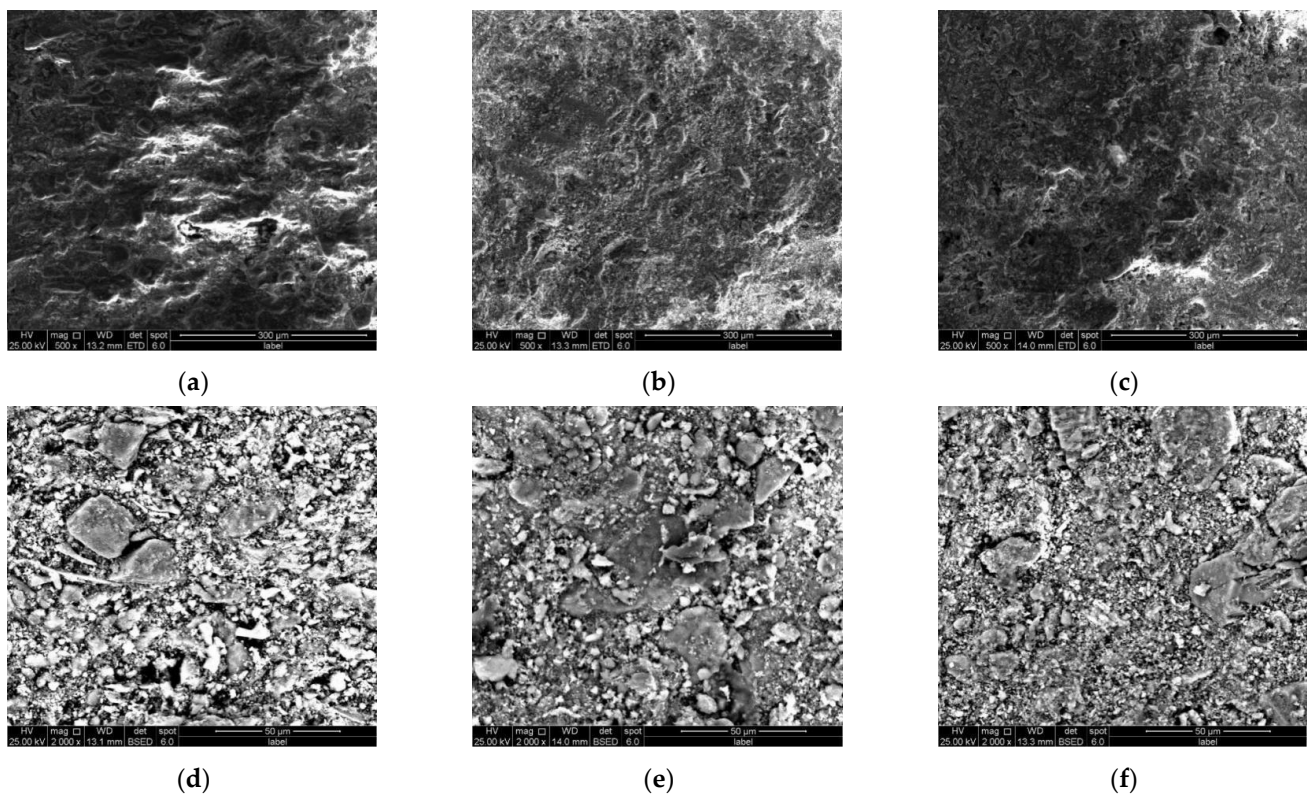


Figure 9. The micro-morphology diagrams of scanning electron microscope: (a) Group X (500 times); (b) Group D (500 times); (c) Group G (500 times); (d) Group X (2000 times); (e) Group D (2000 times); (f) Group G (2000 times).

From Figure 9a,d, it can be seen that the surface particles of the blank group are different in size, the contact mode between the larger particles is mainly point-to-point contacts, and the boundaries between the larger particles are obvious. From Figure 9b,e, it can be found that, compared with the blank group, the contact between the small particles on the surface of the sample in Group D is closer, and the boundary between the larger particles is no longer so obvious; the contact area between the particles on the surface of the sample is changed to be mainly surface contacts. This may be due to the fact that after the hydrolysis reaction between alkoxy and water, silanol is generated, which is condensed

with the active hydroxyl groups on the surface of the stone or around the capillary to form -Si-O-Si- bonds, which connect loose particles to achieve the purpose of reinforcement. Figure 9c,f shows that the surface of Group G sample is still formed by irregular particles, and no uniformly distributed thin film is formed on the surface of the sample, and the microstructure of the sample is basically unchanged by nano-materials.

2. X-ray Diffraction Test

The XRD diffraction patterns of the blank group sample and the Group G sample are shown in Figure 10.

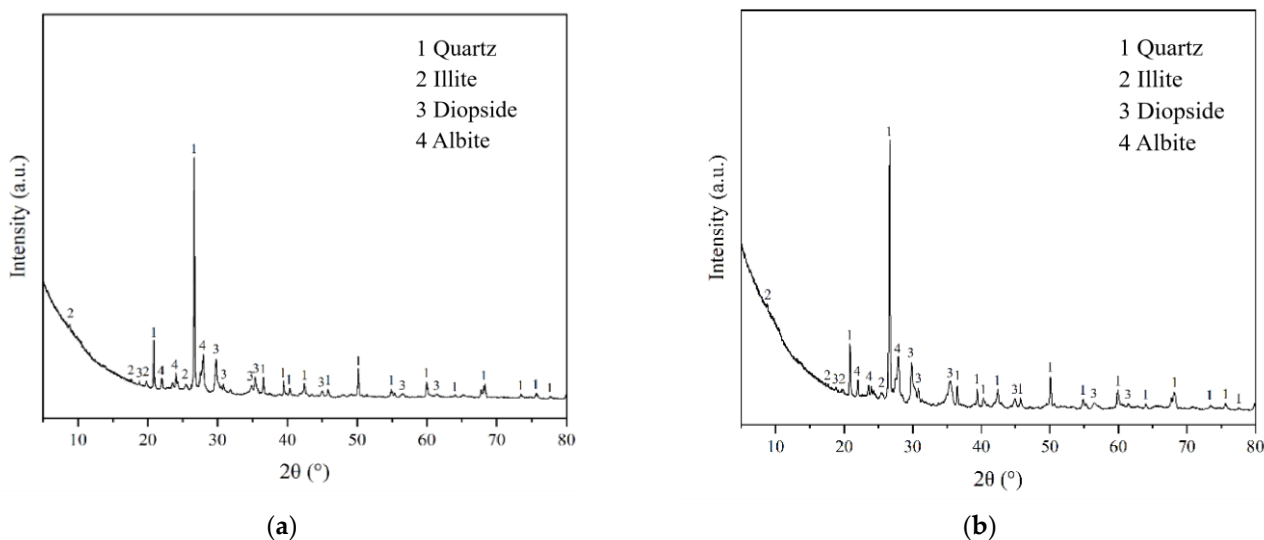


Figure 10. XRD diffraction patterns of the samples: (a) The blank group samples; (b) The G group samples.

The main substance in the blank sample is quartz, and the peaks of illite, diopside, and albite appear in the spectrum, which means that the bricks of the Zhouqiao site contain illite, diopside and albite. By comparing the XRD diffraction patterns of the samples before and after coating with nano-silica-methyltrimethoxysilane hydrolysate, it is found that the diffraction patterns of the two samples basically coincide, quartz with the highest diffraction peak is contained in the brick itself, and no new diffraction peak or diffraction characteristic value appear in the patterns. It can be seen that coating nano-silica-methyltrimethoxysilane hydrolysate will not change the main mineral composition of the bricks.

4. Conclusions

In this study, we preliminarily discussed the properties and anti-weathering protection effects of five basic materials and three nano-composites. This was performed through various tests including the pH test, color difference test, salt tolerance cycling test, water absorption test, air permeability test, ultraviolet radiation resistance test and microscopic test. According to the analysis of the experimental results of this study, it is considered that the anti-weathering resistance of basic materials is improved after doping nano-silica. This improvement addresses the deficiency of a single material in the anti-weathering resistance of masonry cultural relics. The main conclusions of this study are as follows:

- (1) Potassium methyl silicate is slightly alkaline, and the color of the sample changes greatly before and after coating. The sample has good salt resistance and waterproof effect, but its air permeability is reduced by 22.96% compared with the blank group, and the material has high transmission and poor radiation protection performance. The pH value of waterborne acrylic emulsion is 8, and the color difference of the sample before and after coating is large. In the salt tolerance cycling test, the sample forms a hard shell of about 1–2 mm on the outermost layer, and after soaking in water for a period of time, an obvious whitening phenomenon will appear in the sample,

with general waterproof effect and the worst air permeability. Nano-titanium dioxide sol has strong acidity, the color of the sample coated with it changes slightly before and after coating, and its salt resistance is poor. After soaking in water, a slight whitening phenomenon will appear in the sample, and its waterproof and air permeability are average, which has a good shielding effect on ultraviolet light.

- (2) The pH values of methyl trimethoxysilane and methyl trimethoxysilane hydrolysate are moderate, and the color changes of the samples before and after coating all meet the requirements for color difference. The salt tolerance of the coated sample improved after the hydrolysis of methyltrimethoxysilane. Compared to the blank group, the water absorption of the two materials is significantly reduced, which can be attributed to the presence of inert hydrophobic groups in alkyl siloxane. The air permeability of the samples for both materials is good, with the latter being better than the former. However, their resistance to ultraviolet radiation is poor.
- (3) The addition of 0.5% nano-silica has little effect on the pH value of basic materials. However, adding an appropriate amount of nano-silica can reduce the color difference for materials that experience a significant decrease in lightness before and after coating. In addition, the air permeability of the basic materials is improved to some extent. After incorporating nano-silica, the transmittance of methyl trimethoxysilane hydrolysate decreased by 90.89% under 365 nm ultraviolet light, indicating improved ultraviolet shielding and absorption capabilities.
- (4) The results of SEM test showed that after coating methyl trimethoxysilane hydrolysate, the surface particles of the sample changed from point contact to surface contact, and the contact was closer, which is because alkoxy groups become silanol after the hydrolysis reaction. It has a condensation reaction with the active hydroxyl groups on the surface of the brick or around the capillary hole to form the -Si-O-Si-bonds, which connect the loose particles for the purpose of reinforcement. By comparing the XRD patterns of samples before and after coating with the nano-composite, it is evident that the masonry of the Zhouqiao site contains mineral components such as illite, diopside, and albite. Furthermore, the application of this nano-composite coating does not alter the primary mineral components of the bricks.

The above research shows that the composite obtained from methyl trimethoxysilane hydrolysate doped with nano-silica has a good performance in the anti-weathering protection of masonry cultural relics, which has a certain reference value for the study of anti-weathering protection of masonry cultural relics. However, it is necessary to further explore the optimal proportion of nano-composites and the enhancement mechanism of anti-weathering resistance by changing the dosage and types of nano-materials.

Author Contributions: Data curation, R.L.; Project administration, Q.M.; Validation, K.C. and X.Z.; Writing—original draft, J.Z. All authors have read and agreed to the published version of the manuscript.

Funding: The research work carried out in this paper has been supported by Special Project of Innovation and Research in Henan Province in 2023 (project number: 23111321100), the key scientific research projects of colleges and universities in Henan Province in 2022 (project number: 22A560018), and the horizontal project of Zhengzhou City Cultural Relic Institute in 2021 (project number: 20211214C). Thank you for the financial support.

Institutional Review Board Statement: Not applicable.

Informed Consent Statement: Not applicable.

Data Availability Statement: Not applicable.

Conflicts of Interest: The authors declare no conflict of interest.

References

1. Li, Q. Analysis, Monitoring, Evaluation and Protection of Ancient Bridge Structure System and Stone Arch Bridge. Master's Thesis, Zhejiang University, Zhejiang, China, 2011.

2. Scherer, G.W.; Flatt, R.; Wheeler, G. Materials Science Research for the Conservation of Sculpture and Monuments. *MRS Bull.* **2001**, *26*, 44–50. [[CrossRef](#)]
3. Song, T.S.; Wang, D.S.; Tian, M. Study on the Influence of Atmospheric Environment on the Lesion Mechanism of Stone Cultural Relics Sites. *J. North China Univ. Sci. Technol.* **2022**, *44*, 86–93.
4. Ma, H. Experiment and Mechanism Study on Strengthening Clay Brick with Hydroxyapatite. Master's Thesis, Anhui University of Science and Technology, Huainan, China, 2018.
5. Liu, Q.; Zhang, B.; Liang, G. Bioinspired Preparation of a Protective Biomineralized Material on the Surfaces of Historic Stones. *Acta Chim. Sinica.* **2006**, *64*, 1601–1605.
6. He, L. Study on Fluoropolymer and Its Protection of Cultural Relics. Ph.D. Thesis, Northwestern Polytechnical University, Xian, China, 2002.
7. Hu, J. The Law of Science and Technology of Protection of Historical Relics. *Sci. Technol. Rev.* **2001**, *4*, 52–55.
8. La Russa, M.F.; Rovella, N.; Alvarez De Buergo, M.; Belfiore, C.M.; Pezzino, A.; Crisci, G.M.; Ruffolo, S.A. Nano-TiO₂ Coatings for Cultural Heritage Protection: The Role of the Binder on Hydrophobic and Self-Cleaning Efficacy. *Prog. Org. Coat.* **2016**, *91*, 1–8. [[CrossRef](#)]
9. Zhang, Z.; Liu, B.; Gao, Y.M. Modification of Aqueous Acrylic Resin by End-vinyl Siloxane. *Mater. Rep.* **2019**, *33*, 519–522.
10. Lin, R.; Liu, C.H.; Lin, Z.W. Research Progress of Modification and Functional Application of Waterborne Acrylic Coating. *Surf. Technol.* **2017**, *46*, 133–140. [[CrossRef](#)]
11. Vishwakarma, A.; Singh, M.; Weclawski, B.; Reddy, V.J.; Kandola, B.K.; Manik, G.; Dasari, A.; Chattopadhyay, S. Construction of Hydrophobic Fire Retardant Coating on Cotton Fabric Using a Layer-by-Layer Spray Coating Method. *Int. J. Biol. Macromol.* **2022**, *223*, 1653–1666. [[CrossRef](#)]
12. Wang, J. Application of Organosilicon Material in the Protection of Stone Cultural Relics against Weathering. *J. Longdong Univ.* **2020**, *31*, 46–50.
13. Chen, Z.; Su, X.; Wu, W.; Chen, S.; Zhang, X.; Wu, Y.; Xie, H.; Li, K. Superhydrophobic PDMS@TiO₂ Wood for Photocatalytic Degradation and Rapid Oil-Water Separation. *Surf. Coat. Technol.* **2022**, *434*, 128182. [[CrossRef](#)]
14. Chen, B.; Pan, Y.; Chen, Y.; Zhang, Z.; Yang, Z.; Zheng, M.; Lu, T.; Jiang, L.; Qian, H. TiO₂ Nanoparticles Exert an Adverse Effect on Aquatic Microbial Communities. *Sci. Total Environ.* **2022**, *831*, 154942. [[CrossRef](#)] [[PubMed](#)]
15. Fistos, T.; Fierascu, I.; Doni, M.; Chican, I.E.; Fierascu, R.C. A Short Overview of Recent Developments in the Application of Polymeric Materials for the Conservation of Stone Cultural Heritage Elements. *Materials* **2022**, *15*, 6294. [[CrossRef](#)] [[PubMed](#)]
16. Frigione, M.; Lettieri, M. Novel Attribute of Organic–Inorganic Hybrid Coatings for Protection and Preservation of Materials (Stone and Wood) Belonging to Cultural Heritage. *Coatings* **2018**, *8*, 319. [[CrossRef](#)]
17. Aslanidou, D.; Karapanagiotis, I.; Lampakis, D. Waterborne Superhydrophobic and Superoleophobic Coatings for the Protection of Marble and Sandstone. *Materials* **2018**, *11*, 585. [[CrossRef](#)]
18. Fruth, V.; Todan, L.; Codrea, C.I.; Poenaru, I.; Petrescu, S.; Aricov, L.; Ciobanu, M.; Jecu, L.; Ion, R.M.; Predoana, L. Multifunctional Composite Coatings Based on Photoactive Metal-Oxide Nanopowders (MgO/TiO₂) in Hydrophobic Polymer Matrix for Stone Heritage Conservation. *Nanomaterials* **2021**, *11*, 2586. [[CrossRef](#)] [[PubMed](#)]
19. Peng, M.; Wang, L.; Guo, L.; Guo, J.; Zheng, L.; Yang, F.; Ma, Z.; Zhao, X. A Durable Nano-SiO₂-TiO₂/Dodecyltrimethoxysilane Superhydrophobic Coating for Stone Protection. *Coatings* **2022**, *12*, 1397. [[CrossRef](#)]
20. Wang, G.; Wei, X.H.; Zhu, J.F. Effect of IBTES-TiO₂@SiO₂ Composite Sol on Hydrophobic Properties of Sandstone Cultural Relics. *Bullettin Chin. Ceram. Soc.* **2022**, *41*, 332–341. [[CrossRef](#)]
21. Shu, H. Study on the Protection of Stone Cultural Relics by TiO₂ Modified Sol Materials. Master's Thesis, Yunnan University, Kunming, China, 2020.
22. Zhang, B.J.; Tie, J.H.; Liu, T. Preventing the Protective Destruction from the Surface Chemical Protection—The Problems and Strategies of the Protective Destruction in the Historic Stone Protection. *Study Cave Temple.* **2010**, 207–213.
23. Chobba, M.B.; Weththimuni, M.L.; Messaoud, M.; Urzi, C.; Bouaziz, J.; De Leo, F.; Licchelli, M. Ag-TiO₂/PDMS Nanocomposite Protective Coatings: Synthesis, Characterization, and Use as a Self-Cleaning and Antimicrobial Agent. *Prog. Org. Coat.* **2021**, *158*, 106342. [[CrossRef](#)]
24. Chen, X.; Huang, Y.; Zhang, L.; Liu, J.; Wang, C.; Wu, M. Cellulose Nanofiber Assisted Dispersion of Hydrophobic SiO₂ Nanoparticles in Water and Its Superhydrophobic Coating. *Carbohydr. Polym.* **2022**, *290*, 119504. [[CrossRef](#)]
25. Qiao, Y.P. Structural Regulation and Performance Evaluation of Ag/Zn Based Antibacterial Agents. Master's Thesis, Yantai University, Yantai, China, 2022.
26. Zhou, Y.Z.; Wang, H.J.; Chen, H. Effects of phosphogypsum modified with potassium methyl silicate on mechanical properties of cement-based wet-mixed mortar. *New Build. Mater.* **2022**, *49*, 123–127.
27. Lv, X.; Qin, Y.; Liang, H.; Han, Y.; Li, J.; He, Y.; Cui, X. Potassium Methyl Silicate (CH₅SiO₃Na) Assisted Activation and Modification of Alkali-Activated-Slag-Based Drying Powder Coating for Protecting Cement Concrete. *Constr. Build. Mater.* **2022**, *326*, 126858. [[CrossRef](#)]
28. Wu, Y. Research and Application on the Shrinkage Characteristics of Natural Hydraulic Lime Grouting Materials for Cultural Preservation. Master's Thesis, Chengdu University of Technology, Chengdu, China, 2018.
29. Li, Y.F.; Xu, L.N.; Fang, X.H. On the Characteristics, Properties and Application of Pure Acrylic Emulsion in the Conservation of Murals. *Res. Conserv. Cave Temples Earthen Sites* **2022**, *1*, 66–78.

30. Yang, T.; Zhang, Z.J.; Xu, D. On the Characteristics, Simulation Study on Penetration and Reinforcement of Alkoxy-silicon-containing Materials in Weathered Sandstone. *Silicone Mater.* **2021**, *35*, 16–23.
31. Xie, Z.B. Study of the protective properties of methyl—Trimethoxysilicane on historic sandstone. *Sci. Conserv. Archaeol.* **2008**, *20*, 10–15+73. [[CrossRef](#)]
32. Zhang, L. Application of AMC-E Acrylate Elastic Gel in Reinforcement of Inferior Fossil Cultural Relics. Master's Thesis, Zhengzhou University, Zhengzhou, China, 2020.
33. Maravelaki-Kalaitzaki, P.; Kallithrakas-Kontos, N.; Korakaki, D.; Agioutantis, Z.; Maurigiannakis, S. Evaluation of Silicon-Based Strengthening Agents on Porous Limestones. *Prog. Org. Coat.* **2006**, *57*, 140–148. [[CrossRef](#)]
34. Wan, Y.B. Selection and Nano-doped of Anti-weathering Materials for Conservation of Historical Sandstones. Master's Thesis, Harbin Institute of Technology, Harbin, China, 2011.
35. WW/T 0028-2010; Test Methods for the Evaluation of Anti-Weathering Materials for the Conservation of the Sandstone Monument. National Cultural Heritage Administration of the People's Republic of China: Beijing, China, 2010.
36. GB/T 17146-2015; Test Methods for Water Vapour Transmission Properties of Building Materials and Products. General Administration of Quality Supervision, Inspection and Quarantine of the People's Republic of China: Beijing, China, 2015.
37. Du, J.H. Research and Development of Theoretical and Experimental Program about Resistant Weathering Materials in Stone Arch Bridge. Master's Thesis, Chongqing Jiaotong University, Chongqing, China, 2011.
38. GB/T 1865-2009; Paints and varnishes-Artificial weathering and exposure to artificial radiation-Exposure to filtered xenon-arc radiation. General Administration of Quality Supervision, Inspection and Quarantine of the People's Republic of China: Beijing, China, 2009.
39. Yang, G.; Deng, A.Z. Effect of topcoat on properties of energy-efficient architectural coating with nickel titanium yellow as pigment. *Electropating Finish.* **2017**, *36*, 966–970. [[CrossRef](#)]
40. Sardon, H.; Irusta, L.; Aguirresarobe, R.H.; Fernández-Berridi, M.J. Polymer/Silica Nanohybrids by Means of Tetraethoxysilane Sol–Gel Condensation onto Waterborne Polyurethane Particles. *Prog. Org. Coat.* **2014**, *77*, 1436–1442. [[CrossRef](#)]
41. Heck, C.A.; Dos Santos, J.H.Z.; Wolf, C.R. Waterborne Polyurethane: The Effect of the Addition or in Situ Formation of Silica on Mechanical Properties and Adhesion. *Int. J. Adhes. Adhes.* **2015**, *58*, 13–20. [[CrossRef](#)]
42. Tao, L. Study on Evaluation Method of Stone Cultural Relics Protection Materials. Master's Thesis, Lanzhou University of Technology, Lanzhou, China, 2010.
43. Li, T.; Fan, Y.; Wang, K.; Song, S.; Liu, X.; Bu, N.; Li, R.; Zhen, Q.; Bashir, S. Methyl-Modified Silica Hybrid Fluorinated Paraloid B-72 as Hydrophobic Coatings for the Conservation of Ancient Bricks. *Constr. Build. Mater.* **2021**, *299*, 123906. [[CrossRef](#)]

Disclaimer/Publisher's Note: The statements, opinions and data contained in all publications are solely those of the individual author(s) and contributor(s) and not of MDPI and/or the editor(s). MDPI and/or the editor(s) disclaim responsibility for any injury to people or property resulting from any ideas, methods, instructions or products referred to in the content.